Environmental Science & Technology Letters

Letter

Cite This: Environ. Sci. Technol. Lett. 2018, 5, 32−37

pubs.acs.org/journal/estlcu

Significant Production of Secondary Organic Aerosol from Emissions of Heated Cooking Oils

Tengyu Liu,[†] Zhaoyi Wang,[‡,§] Dan Dan Huang,[†] Xinming Wang,[*,‡,∥] and Chak K. Chan[*,†]

[†]School of Energy and Environment, City University of Hong Kong, Hong Kong, China

[‡]State Key Laboratory of Organic Geochemistry and Guangdong Key Laboratory of Environmental Protection and Resources Utilization, Guangzhou Institute of Geochemistry, Chinese Academy of Sciences, Guangzhou 510640, China

[§]University of Chinese Academy of Sciences, Beijing 100049, China

[∥]Center for Excellence in Urban Atmospheric Environment, Institute of Urban Environment, Chinese Academy of Sciences, Xiamen 361021, China

Supporting Information

ABSTRACT: Cooking emissions have been identified as a major source of primary organic aerosol (POA) in urban environments. Cooking may also be a potential source of secondary organic aerosol (SOA) because of the abundant emissions of non-methane organic gases. We studied SOA formation from the photooxidation of emissions from seven vegetable oils heated at 200 °C under high-NO_x conditions in a smog chamber. After the samples had been aged under an OH exposure of 1.0×10^{10} molecules cm^{-3} s, the SOA formation rate was generally 1 order of magnitude higher than the POA emission rate. We determined that alkenals, which are not traditional SOA precursors in chemical transport models, accounted for 5−34% of the observed SOA. The unexplained SOA may be attributed to the oxidation of primary semivolatile and intermediate-volatility organic compounds (SVOCs and IVOCs, respectively), which were estimated to contribute an additional 9−106% of the observed SOA assuming the volatility distribution of heated cooking oils is the same as that of vehicle exhaust. Our results suggest that cooking can potentially be an important source of SOA in urban areas and that there is a need to characterize both SVOCs and IVOCs emitted from cooking and their SOA yields.

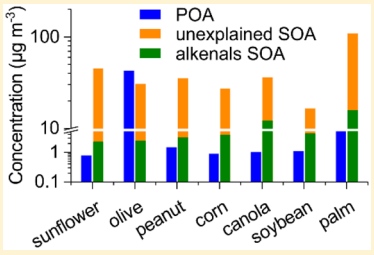

1. INTRODUCTION

Organic aerosol (OA), which comprises both primary and secondary organic aerosol (POA and SOA, respectively), has important impacts on air quality, climate, and human health.[1] SOA is formed via the oxidation of organic gases,[1] and the mass concentration of SOA often exceeds the amount of POA emitted directly from sources, even in urban areas.[2,3] However, our limited knowledge of sources and the mechanism of formation of SOA generally leads to large discrepancies between modeled and measured SOA concentrations[4−6] and therefore severely impedes our understanding of climate and health effects of SOA.

Cooking is an important source of POA in urban areas[7−13] and can potentially form SOA, as cooking emits SOA precursors such as alkenals ($<C_{10}$)[14−16] and primary semivolatile and intermediate-volatility organic compounds (SVOCs and IVOCs, respectively; e.g., $\geq C_{13}$ *n*-alkanes, *n*-alkanals, and fatty acids).[16−18] Assuming that cooking emissions have volatility distributions of SVOCs and IVOCs and SOA yields that are the same as those of vehicle exhaust, Hayes et al.[19] showed via modeling that SVOCs and IVOCs from cooking emissions contributed 19−35% of the SOA mass in downtown Los Angeles. Recent laboratory studies have also demonstrated SOA formation from gas-phase emissions of heated cooking oils[20] and meat charbroiling.[21] However, the SOA formation potential, relative POA and SOA contributions, and main SOA precursors related to cooking remain highly uncertain.

Frying with vegetable oils is a common cooking technique in numerous cultures,[22] and heated cooking oils can produce large amounts of particles[23,24] and organic gases.[15,16] In this work, we investigate the formation of SOA from the photooxidation of emissions from heated cooking oils under high-NO_x conditions in a smog chamber. The objectives of this study are to identify the main SOA precursors, estimate the SOA formation potential, and evaluate the relative contributions of emissions of heated cooking oil to POA and SOA.

2. MATERIALS AND METHODS

2.1. Smog Chamber Experiments. Photooxidation experiments were performed on emissions from seven cooking oils, including sunflower, olive, peanut, corn, canola (rapeseed), soybean, and palm oils, in a 30 m^3 indoor smog chamber at the Guangzhou Institute of Geochemistry, Chinese Academy of Sciences (GIG-CAS)[25−27] (Table 1; see more details in the Supporting Information); these cooking oil types constituted

Received: November 22, 2017
Revised: December 7, 2017
Accepted: December 11, 2017
Published: December 11, 2017

Table 1. Experimental Conditions and Results of the Photooxidation Experiments

cooking oil	$[NMOG]_0$[a] (ppb)	$[NO]_0$[a,b] (ppb)	$[NO_2]_0$[a,b] (ppb)	[NMOG]:[NO_x] (ppbC:ppb)	$[AS]_0$[a] ($\mu g\ m^{-3}$)	[POA][c] ($\mu g\ m^{-3}$)	OH exposure ($\times 10^{10}$ molecules cm^{-3} s)	[SOA][d] ($\mu g\ m^{-3}$)	effective SOA yield
sunflower	352	167	248	4.9	23.3	0.8	1.0 ± 0.16	45.0	0.50
olive	262	173	185	4.0	42.6	42.3	1.3 ± 0.14	30.6	0.31
peanut	219	273	246	2.6	66.5	1.4	2.1 ± 0.15	35.0	0.28
corn	216	199	206	3.2	71.5	0.9	1.8 ± 0.15	27.1	0.18
canola	595	293	243	5.4	58.4	1.0	3.5 ± 0.20	36.2	0.07
soybean	257	246	205	3.4	55.8	1.1	1.7 ± 0.081	16.4	0.10
palm	1392	232	194	18.9	59.4	9.3	1.3 ± 0.064	107.5	0.16

[a]Mass concentrations when black lights were turned on. [b]As measured by a chemiluminescence NO_x monitor. Note the interference of HONO in NO_x measurements. [c]The concentration of POA was determined after the introduction of emissions from heated cooking oils. [d]The wall-loss-corrected concentration of SOA was determined at the end of the experiment. For peanut, corn, canola, and soybean oils, the $\omega = 1$ method[41−43] was used to correct particle wall loss. For sunflower, olive, and palm oils, the $\omega = 0$ method[41,42] was used.

>90% of the global consumption of vegetable oils.[28] All experiments were conducted at 25 °C and a relative humidity (RH) of <5%. Ammonium sulfate (AS) seed particles were introduced into the chamber by an atomizer followed by a diffusion dryer. These seed particles, which had a geometric mean diameter of approximately 120 nm, served as condensation sinks to reduce organic vapor wall loss.[29]

After the injection of seed particles, 250 mL of vegetable oil was heated at approximately 200 °C, which is below the smoke point of all of the oils studied and representative of typical cooking temperatures,[30,31] for 1−1.5 h in a 500 mL flask in a dimethyl silicone oil bath. Emissions were introduced into the chamber via an air stream passing through a 2 m Teflon tube heated to 70 °C. The residence time in the transfer line was <1 s, resulting in particle number wall losses of <3%, according to Liu et al.[32]

Nitrous acid (HONO) was then introduced into the chamber as a source of hydroxyl radical (OH) following the methods of Ng et al.[33] The initial ratio of non-methane organic gases (NMOGs) to NO_x (NMOG:NO_x) typically fell between 2.6 and 5.4 ppbC:ppb, except for the palm oil experiment, in which it measured 18.9 ppbC:ppb. These ratios were higher than the typical urban level of ~3.[34] After all gases and particles had been well mixed, the emissions were exposed to black lights (60 W Philips/10R BL, Royal Dutch Philips Electronics Ltd., Amsterdam, The Netherlands) for 2.0−4.5 h. A control experiment without emissions from heated cooking oils was also conducted to characterize the contribution of matrix gases and residual pollutants in the transfer line between the oil flask and the chamber, and the concentration of SOA formed in this experiment was <0.1 $\mu g\ m^{-3}$.

2.2. Characterization of Gas- and Particle-Phase Chemical Compositions. NMOGs were sampled through a heated line (70 °C) followed by a filter to remove particles and characterized using a commercial proton-transfer-reaction time-of-flight mass spectrometer (PTR-TOF-MS, model 2000, H_3O^+ reagent ion, Ionicon Analytik GmbH, Innsbruck, Austria).[35,36] The observed NMOG masses were assigned to the most likely compounds on the basis of online and offline analyses of NMOG emissions from heated cooking oils.[14−16,37] Fragmentation patterns of aldehydes were estimated from literature data[16,38] and applied to the fragmentation corrections (Table S1). More detailed descriptions of operation conditions, calibrations, and fragmentation corrections are provided in the Supporting Information. Chamber OH concentrations were determined from the decay of acrolein or heptenal[21,26] (Figure S1; see the Supporting Information for details).

A scanning mobility particle sizer (SMPS, TSI Inc., classifier model 3080, CPC model 3775) was used to measure particle number concentrations and size distributions. Nonrefractory components, including organics, nitrate, sulfate, and ammonium, were chemically characterized using a high-resolution time-of-flight aerosol mass spectrometer (hereafter AMS, Aerodyne Research Inc.)[39] (see the Supporting Information for further details). Using the method of Farmer et al.,[40] we found that all nitrates formed were organic nitrates in our experiments.

2.3. Data Analysis. Particle wall loss is typically corrected by assuming that organic vapors condense solely on suspended particles ($\omega = 0$)[41,42] or remain in equilibrium with both wall-bound and suspended particles ($\omega = 1$).[41−43] The $\omega = 1$ method was used for experiments involving OA internally mixed with AS seed particles (peanut, corn, canola, and soybean oil experiments). The wall-loss-corrected SOA concentration was calculated using the following equation:

$$[SOA]_t = \frac{[OA]_{sus,t}}{[AS]_{sus,t}}[AS]_{sus,0} - [OA]_{sus,0} \quad (1)$$

where $[OA]_{sus,t}$ and $[AS]_{sus,t}$ are the concentrations of suspended OA and AS seed particles, respectively, measured by the AMS at time t. $[OA]_{sus,0}$ and $[AS]_{sus,0}$ are the concentrations of suspended OA and AS seed particles at the time when the black lights were turned on, respectively, and these values were determined from the particle volume concentration measured by the SMPS and the ratio of $[OA]_{sus,0}$ to $[AS]_{sus,0}$ measured by the AMS. Densities of 1.77 $g\ cm^{-3}$,[33] 1.0 $g\ cm^{-3}$,[21] and 1.4 $g\ cm^{-3}$,[20] were assumed for AS, POA, and SOA, respectively, for the conversion of particle volume to mass. For the $\omega = 0$ method, the particle wall loss rate constant was determined by fitting an exponential decay to the SMPS volume concentration for the period after SOA production completed. This wall loss rate constant was then applied to the entire experiment to correct for particle wall loss.[42] Application of the $\omega = 0$ method to these same experiments yielded a <10% difference in the wall-loss-corrected SOA concentrations compared with those of the $\omega = 1$ method. This small difference is similar to that reported by Chacon-Madrid and Donahue[44] and Trump et al.[45] for fast oxidation of long-chain *n*-alkanes, *n*-ketones, *n*-aldehydes, and α-pinene. For the other experiments, in which OA was externally mixed with AS seed particles (sunflower, olive, and palm oil experiments), the $\omega = 1$ method cannot be used.[42] Because the use of $\omega = 1$ and $\omega = 0$ methods did not yield significant differences in the internal mixture experiments

DOI: 10.1021/acs.estlett.7b00530
Environ. Sci. Technol. Lett. 2018, 5, 32−37

discussed above, we assumed the $\omega = 0$ method to be suitable for wall loss corrections in experiments involving externally mixed particles.

The emission rates (ERs, μg min^{-1}) of NMOG and POA and the production rate (PR, μg min^{-1}) of SOA were calculated using the following equation:[16,20,46]

$$\text{ER or PR} = [\text{P}] \times \text{DR} \times F \quad (2)$$

where [P] is the NMOG, POA, or SOA concentration in μg m^{-3}, DR is the dilution ratio, and F is the flow rate of cooking emission carrier gas in m^3 min^{-1}.

3. RESULTS AND DISCUSSION

3.1. SOA Production. Figure 1a shows the NMOG ERs from different heated cooking oils. These NMOGs were

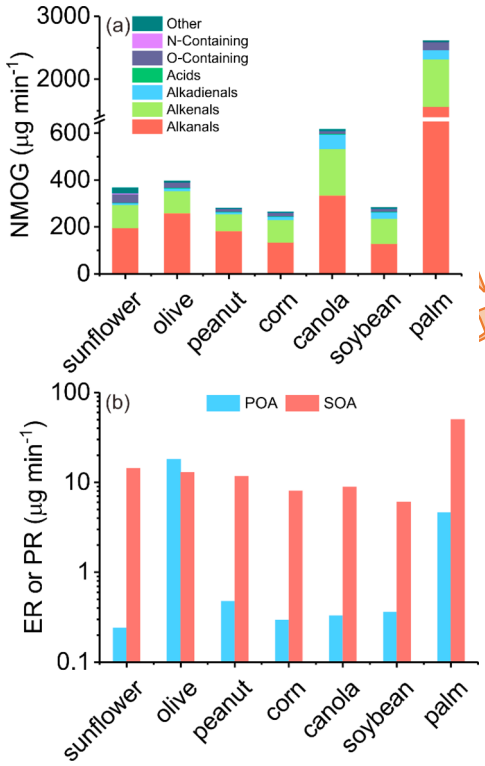

Figure 1. (a) Emission rates of NMOGs from different heated cooking oils. (b) POA emission rates and SOA production rates for different heated cooking oils. SOA production rates were determined after the emissions were exposed to OH of 1.0×10^{10} molecules cm^{-3} s.

classified into seven families on the basis of their molecular characteristics. Alkanals, alkenals, and alkadienals dominated the NMOG emissions, which is consistent with previous studies.[14−16] In general, the PTR-TOF-MS detects the majority of VOCs from heated cooking oils; undetected alkanes, which are known not to form SOA, have been reported to contribute <5% of the total NMOG mass from cooking with seed oils.[17] Typically, the contributions of other isomers, such as ketones, are negligible, and only one aldehyde isomer is present for a specific molecular formula.[14−16] Therefore, we assume that the contributions of other isomers were negligible in our experiments considering the current experimental limitation in identifying isomers. Heated palm oil had the highest NMOG emissions, followed by canola, olive, and sunflower oils, while peanut, corn, and soybean oils had the lowest NMOG emissions. The different emission patterns for different cooking oils (Figure S2) may be explained by varying oil triglyceride compositions.[47]

The amounts of SOA formed from the photochemical aging of emissions from heated cooking oils were substantial, generally exceeding the amounts of POA emitted (Table 1). Figure 1b shows the POA ERs and SOA PRs for different cooking oils. POA ERs were determined after the introduction of emissions from heated cooking oils. SOA PRs were determined at an OH exposure of 1.0×10^{10} molecules cm^{-3} s, which corresponds to 1.9 h of photochemical age, assuming 24 h average ambient OH concentrations of 1.5×10^6 molecules cm^{-3}.[48] Figure S3 shows that the POA ERs were not correlated with the cooking oil smoke points. The SOA PRs were 6−50 μg min^{-1} and ranged from 0.7 times the POA ER for olive oil to 60 times the POA ER for sunflower oil. Heated palm oil had the highest SOA PR, followed by sunflower and olive oils. When POA was included, palm oil still had the highest OA ER, but the OA ER for olive oil exceeded that for sunflower oil.

These PRs were 1−2 orders of magnitude higher than the SOA PRs from gas-phase emissions from the same cooking oils after approximately 5 h of photochemical aging in our earlier study.[20] Liu et al.[20] stated that filtration of the POA prior to introduction to the flow reactor removed a large fraction of the SVOCs and IVOCs. In addition, the aging experiments of Liu et al.[20] were conducted in the absence of NO_x, which has been found to enhance the formation of SOA from aldehydes.[49] Both factors may have contributed to the SOA PR discrepancy between the two studies.

3.2. Contributions of Individual NMOGs to Observed SOA. The concentrations of SOA formed from individual NMOGs were estimated from the reacted NMOG mass at a certain OH exposure and the corresponding SOA yield obtained from the literature.[49,50] The OH-reaction rate constants and the applied SOA yields of precursors used in the calculation are listed in Tables S2 and S3 and discussed in detail in the Supporting Information. Although alkanals contributed a large fraction of the NMOG emissions (Figure 1a and Figure S2), <C_{11} alkanals were not included in the calculation because of their negligible SOA mass yields.[51] The concentrations of all traditional SOA precursors included in typical SOA models, i.e., isoprene, aromatics, and monoterpenes, were below the PTR-TOF-MS detection limit; therefore, these species were also excluded from the estimates. Figure 2 shows the estimated contributions of 10 individual alkenals to the observed SOA. The circles and triangles denote the lowest and highest estimates, respectively, based on the lowest and highest SOA yields. Over all experiments, these alkenals accounted for 5−34% of the observed SOA; they would account for 8−55% of SOA if the highest yield estimates were used. These alkenals resulted in effective yields ranging from 0.07 to 0.50.

Figure 2 also shows that the contributions of individual alkenals to observed SOA were highly variable for different cooking oils. Acrolein, hexenal, and heptadienal altogether contributed to 26 and 17% of the observed SOA for canola and soybean oils, respectively; however, they contributed only to 4, 4, and 8% of the observed SOA for olive, peanut, and corn oils, respectively. The unexplained SOA may be attributed to the oxidation of unspeciated SVOCs and IVOCs, which have been recognized as important precursors for biomass burning[52,53] and vehicle exhaust[43,54,55] SOA. *n*-Alkanes, *n*-alkanals, and fatty

DOI: 10.1021/acs.estlett.7b00530
Environ. Sci. Technol. Lett. 2018, 5, 32−37

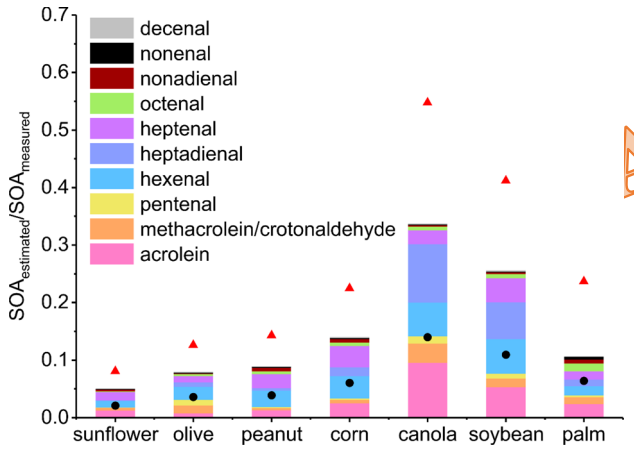

Figure 2. Estimated contribution of 10 individual alkenals to observed SOA for each heated cooking oil. Contributions were determined at the end of each experiment. Circles and triangles represent the contributions applying the lowest and highest SOA yields, respectively, for each SOA precursor.

acids ($\geq C_{13}$) falling in the SVOC and IVOC range have been observed in emissions from cooking with seed oils[17] and meat charbroiling.[18] By assuming that the volatility distribution of heated cooking oils was similar to that of diesel exhaust[54] and that the concentrations of IVOCs were 1.5 times the total mass of POA plus SVOCs[5,54] (see details in the Supporting Information), we estimated that SVOCs and IVOCs contributed 9−106% of the observed SOA, leaving a large fraction of SOA still unexplained (Figure S4). It is possible that the volatility distributions of diesel exhaust and IVOC and SVOC surrogates C_{13} *n*-alkane and C_{23} *n*-alkane may not be representative of cooking oils.[20] Future work should focus on characterizing SVOCs and IVOCs from cooking to better constrain the resulting formation of SOA.

3.3. Atmospheric Implications. We observed that the rate of generation of SOA from emissions of heated cooking oils was 1 order of magnitude higher than that of POA after 1.9 h of equivalent photooxdiation in the presence of NO_x. To the best of our knowledge, this is the first time that SOA formed from emissions of heated cooking oil exceeding its POA has been reported, under OH exposures lower than real atmospheric conditions. The NMOG:NO_x ratios, which were higher than typical urban ratios, may to some extent underestimate SOA formation, as a high level of NO_x could enhance the formation of SOA from aldehydes.[49] Further studies of the NO_x dependence of SOA from cooking are needed. In addition, we solely studied heated cooking oils; other cooking processes, such as boiling and frying food, also likely produce substantial SOA. Given that POA from cooking has been found to contribute 10−34.6% of the total OA in urban areas,[7−13] cooking may also be an important source of SOA in urban areas. In recent years, increasingly strict vehicular emission control regulations have led to large reductions in SOA from vehicle exhaust in some regions, such as the United States.[43] Our findings suggest that the potential relative contributions of cooking emissions to SOA may increase with time and should also be subject to strict regulations.

■ ASSOCIATED CONTENT

Supporting Information

The Supporting Information is available free of charge on the ACS Publications website at DOI: 10.1021/acs.estlett.7b00530.

Descriptions of smog chamber experiments (Text S1), NMOG measurements (Text S2), OH concentration determinations (Text S3), nonrefractory component measurements (Text S4), production of SOA from NMOG (Text S5), production of SOA from SVOCs and IVOCs (Text S6), a fragmentation table for the most abundant aldehydes (Table S1), alkenal OH reaction rate constants (Table S2), applied SOA yield data (Table S3), $\ln([\text{acrolein}]_0/[\text{acrolein}]_t)$ versus time *t* (Figure S1), relative contributions of different compounds to the total NMOG (Figure S2), POA ERs versus smoke points of different cooking oils (Figure S3), and estimated contributions of NMOGs to the observed SOA (Figure S4) (PDF)

■ AUTHOR INFORMATION

Corresponding Authors

*School of Energy and Environment, City University of Hong Kong, Hong Kong 999077, China. Telephone: +852-34425593. Fax: +852-34420688. E-mail: Chak.K.Chan@cityu.edu.hk.

*State Key Laboratory of Organic Geochemistry, Guangzhou Institute of Geochemistry, Chinese Academy of Sciences, Guangzhou 510640, China. Telephone: +86-20-85290180. Fax: +86-20-85290706. E-mail: wangxm@gig.ac.cn.

ORCID

Tengyu Liu: 0000-0002-3137-5898

Dan Dan Huang: 0000-0003-2878-7469

Xinming Wang: 0000-0002-1982-0928

Notes

The authors declare no competing financial interest.

■ ACKNOWLEDGMENTS

C.K.C. acknowledges the support of the National Natural Science Foundation of China (Project 41675117) and the startup fund of City University of Hong Kong (Grant SGP 9380078). X.W. acknowledges the support of the Strategic Priority Research Program of the Chinese Academy of Sciences (Grant XDB05010200).

■ REFERENCES

(1) Hallquist, M.; Wenger, J. C.; Baltensperger, U.; Rudich, Y.; Simpson, D.; Claeys, M.; Dommen, J.; Donahue, N. M.; George, C.; Goldstein, A. H.; Hamilton, J. F.; Herrmann, H.; Hoffmann, T.; Iinuma, Y.; Jang, M.; Jenkin, M. E.; Jimenez, J. L.; Kiendler-Scharr, A.; Maenhaut, W.; McFiggans, G.; Mentel, T. F.; Monod, A.; Prévôt, A. S. H.; Seinfeld, J. H.; Surratt, J. D.; Szmigielski, R.; Wildt, J. The formation, properties and impact of secondary organic aerosol: current and emerging issues. *Atmos. Chem. Phys.* **2009**, *9* (14), 5155−5236.

(2) Zhang, Q.; Jimenez, J. L.; Canagaratna, M. R.; Allan, J. D.; Coe, H.; Ulbrich, I.; Alfarra, M. R.; Takami, A.; Middlebrook, A. M.; Sun, Y. L.; Dzepina, K.; Dunlea, E.; Docherty, K.; DeCarlo, P. F.; Salcedo, D.; Onasch, T.; Jayne, J. T.; Miyoshi, T.; Shimono, A.; Hatakeyama, S.; Takegawa, N.; Kondo, Y.; Schneider, J.; Drewnick, F.; Borrmann, S.; Weimer, S.; Demerjian, K.; Williams, P.; Bower, K.; Bahreini, R.; Cottrell, L.; Griffin, R. J.; Rautiainen, J.; Sun, J. Y.; Zhang, Y. M.; Worsnop, D. R. Ubiquity and dominance of oxygenated species in organic aerosols in anthropogenically-influenced Northern Hemisphere midlatitudes. *Geophys. Res. Lett.* **2007**, *34* (13), L13801.

(3) Jimenez, J. L.; Canagaratna, M. R.; Donahue, N. M.; Prevot, A. S. H.; Zhang, Q.; Kroll, J. H.; DeCarlo, P. F.; Allan, J. D.; Coe, H.; Ng, N. L.; Aiken, A. C.; Docherty, K. S.; Ulbrich, I. M.; Grieshop, A. P.; Robinson, A. L.; Duplissy, J.; Smith, J. D.; Wilson, K. R.; Lanz, V. A.; Hueglin, C.; Sun, Y. L.; Tian, J.; Laaksonen, A.; Raatikainen, T.; Rautiainen, J.; Vaattovaara, P.; Ehn, M.; Kulmala, M.; Tomlinson, J. M.; Collins, D. R.; Cubison, M. J.; Dunlea, J.; Huffman, J. A.; Onasch, T. B.; Alfarra, M. R.; Williams, P. I.; Bower, K.; Kondo, Y.; Schneider, J.; Drewnick, F.; Borrmann, S.; Weimer, S.; Demerjian, K.; Salcedo, D.; Cottrell, L.; Griffin, R.; Takami, A.; Miyoshi, T.; Hatakeyama, S.; Shimono, A.; Sun, J. Y.; Zhang, Y. M.; Dzepina, K.; Kimmel, J. R.; Sueper, D.; Jayne, J. T.; Herndon, S. C.; Trimborn, A. M.; Williams, L. R.; Wood, E. C.; Middlebrook, A. M.; Kolb, C. E.; Baltensperger, U.; Worsnop, D. R. Evolution of Organic Aerosols in the Atmosphere. *Science* **2009**, *326* (5959), 1525−1529.

(4) de Gouw, J. A.; Middlebrook, A. M.; Warneke, C.; Goldan, P. D.; Kuster, W. C.; Roberts, J. M.; Fehsenfeld, F. C.; Worsnop, D. R.; Canagaratna, M. R.; Pszenny, A. A. P.; Keene, W. C.; Marchewka, M.; Bertman, S. B.; Bates, T. S. Budget of organic carbon in a polluted atmosphere: Results from the New England Air Quality Study in 2002. *J. Geophys. Res.* **2005**, *110* (D16), D16305.

(5) Hodzic, A.; Jimenez, J. L.; Madronich, S.; Canagaratna, M. R.; DeCarlo, P. F.; Kleinman, L.; Fast, J. Modeling organic aerosols in a megacity: potential contribution of semi-volatile and intermediate volatility primary organic compounds to secondary organic aerosol formation. *Atmos. Chem. Phys.* **2010**, *10* (12), 5491−5514.

(6) Volkamer, R.; Jimenez, J. L.; San Martini, F.; Dzepina, K.; Zhang, Q.; Salcedo, D.; Molina, L. T.; Worsnop, D. R.; Molina, M. J. Secondary organic aerosol formation from anthropogenic air pollution: Rapid and higher than expected. *Geophys. Res. Lett.* **2006**, *33* (17), L17811.

(7) Allan, J. D.; Williams, P. I.; Morgan, W. T.; Martin, C. L.; Flynn, M. J.; Lee, J.; Nemitz, E.; Phillips, G. J.; Gallagher, M. W.; Coe, H. Contributions from transport, solid fuel burning and cooking to primary organic aerosols in two UK cities. *Atmos. Chem. Phys.* **2010**, *10* (2), 647−668.

(8) Sun, Y. L.; Zhang, Q.; Schwab, J. J.; Demerjian, K. L.; Chen, W. N.; Bae, M. S.; Hung, H. M.; Hogrefe, O.; Frank, B.; Rattigan, O. V.; Lin, Y. C. Characterization of the sources and processes of organic and inorganic aerosols in New York city with a high-resolution time-of-flight aerosol mass apectrometer. *Atmos. Chem. Phys.* **2011**, *11* (4), 1581−1602.

(9) Crippa, M.; DeCarlo, P. F.; Slowik, J. G.; Mohr, C.; Heringa, M. F.; Chirico, R.; Poulain, L.; Freutel, F.; Sciare, J.; Cozic, J.; Di Marco, C. F.; Elsasser, M.; Nicolas, J. B.; Marchand, N.; Abidi, E.; Wiedensohler, A.; Drewnick, F.; Schneider, J.; Borrmann, S.; Nemitz, E.; Zimmermann, R.; Jaffrezo, J. L.; Prévôt, A. S. H.; Baltensperger, U. Wintertime aerosol chemical composition and source apportionment of the organic fraction in the metropolitan area of Paris. *Atmos. Chem. Phys.* **2013**, *13* (2), 961−981.

(10) Lee, B. P.; Li, Y. J.; Yu, J. Z.; Louie, P. K. K.; Chan, C. K. Characteristics of submicron particulate matter at the urban roadside in downtown Hong Kong—Overview of 4 months of continuous high-resolution aerosol mass spectrometer measurements. *J. Geophys. Res.: Atmos.* **2015**, *120* (14), 7040.

(11) Sun, Y. L.; Zhang, Q.; Schwab, J. J.; Chen, W. N.; Bae, M. S.; Hung, H. M.; Lin, Y. C.; Ng, N. L.; Jayne, J.; Massoli, P.; Williams, L. R.; Demerjian, K. L. Characterization of near-highway submicron aerosols in New York City with a high-resolution aerosol mass spectrometer. *Atmos. Chem. Phys.* **2012**, *12* (4), 2215−2227.

(12) Mohr, C.; DeCarlo, P. F.; Heringa, M. F.; Chirico, R.; Slowik, J. G.; Richter, R.; Reche, C.; Alastuey, A.; Querol, X.; Seco, R.; Peñuelas, J.; Jiménez, J. L.; Crippa, M.; Zimmermann, R.; Baltensperger, U.; Prévôt, A. S. H. Identification and quantification of organic aerosol from cooking and other sources in Barcelona using aerosol mass spectrometer data. *Atmos. Chem. Phys.* **2012**, *12* (4), 1649−1665.

(13) Ge, X.; Setyan, A.; Sun, Y.; Zhang, Q. Primary and secondary organic aerosols in Fresno, California during wintertime: Results from high resolution aerosol mass spectrometry. *J. Geophys. Res.: Atmos.* **2012**, *117* (D19), D19301.

(14) Fullana, A.; Carbonell-Barrachina, A. A.; Sidhu, S. Comparison of Volatile Aldehydes Present in the Cooking Fumes of Extra Virgin Olive, Olive, and Canola Oils. *J. Agric. Food Chem.* **2004**, *52* (16), 5207−5214.

(15) Katragadda, H. R.; Fullana, A.; Sidhu, S.; Carbonell-Barrachina, Á. A. Emissions of volatile aldehydes from heated cooking oils. *Food Chem.* **2010**, *120* (1), 59−65.

(16) Klein, F.; Platt, S. M.; Farren, N. J.; Detournay, A.; Bruns, E. A.; Bozzetti, C.; Daellenbach, K. R.; Kilic, D.; Kumar, N. K.; Pieber, S. M.; Slowik, J. G.; Temime-Roussel, B.; Marchand, N.; Hamilton, J. F.; Baltensperger, U.; Prévôt, A. S. H.; El Haddad, I. Characterization of Gas-Phase Organics Using Proton Transfer Reaction Time-of-Flight Mass Spectrometry: Cooking Emissions. *Environ. Sci. Technol.* **2016**, *50* (3), 1243−1250.

(17) Schauer, J. J.; Kleeman, M. J.; Cass, G. R.; Simoneit, B. R. T. Measurement of Emissions from Air Pollution Sources. 4. C1−C27 Organic Compounds from Cooking with Seed Oils. *Environ. Sci. Technol.* **2002**, *36* (4), 567−575.

(18) Louvaris, E. E.; Karnezi, E.; Kostenidou, E.; Kaltsonoudis, C.; Pandis, S. N. Estimation of the volatility distribution of organic aerosol combining thermodenuder and isothermal dilution measurements. *Atmos. Meas. Technol. Discuss.* **2017**, *2017*, 1−22.

(19) Hayes, P. L.; Carlton, A. G.; Baker, K. R.; Ahmadov, R.; Washenfelder, R. A.; Alvarez, S.; Rappenglück, B.; Gilman, J. B.; Kuster, W. C.; de Gouw, J. A.; Zotter, P.; Prévôt, A. S. H.; Szidat, S.; Kleindienst, T. E.; Offenberg, J. H.; Ma, P. K.; Jimenez, J. L. Modeling the formation and aging of secondary organic aerosols in Los Angeles during CalNex 2010. *Atmos. Chem. Phys.* **2015**, *15* (10), 5773−5801.

(20) Liu, T.; Li, Z.; Chan, M.; Chan, C. K. Formation of secondary organic aerosols from gas-phase emissions of heated cooking oils. *Atmos. Chem. Phys.* **2017**, *17* (12), 7333−7344.

(21) Kaltsonoudis, C.; Kostenidou, E.; Louvaris, E.; Psichoudaki, M.; Tsiligiannis, E.; Florou, K.; Liangou, A.; Pandis, S. N. Characterization of fresh and aged organic aerosol emissions from meat charbroiling. *Atmos. Chem. Phys.* **2017**, *17* (11), 7143−7155.

(22) Abdullahi, K. L.; Delgado-Saborit, J. M.; Harrison, R. M. Emissions and indoor concentrations of particulate matter and its specific chemical components from cooking: A review. *Atmos. Environ.* **2013**, *71*, 260−294.

(23) Torkmahalleh, M. A.; Goldasteh, I.; Zhao, Y.; Udochu, N. M.; Rossner, A.; Hopke, P. K.; Ferro, A. R. PM2.5 and ultrafine particles emitted during heating of commercial cooking oils. *Indoor Air* **2012**, *22* (6), 483−491.

(24) Gao, J.; Cao, C. S.; Wang, L.; Song, T. H.; Zhou, X.; Yang, J.; Zhang, X. Determination of Size-Dependent Source Emission Rate of Cooking-Generated Aerosol Particles at the Oil-Heating Stage in an Experimental Kitchen. *Aerosol Air Qual. Res.* **2013**, *13* (2), 488−496.

(25) Wang, X.; Liu, T.; Bernard, F.; Ding, X.; Wen, S.; Zhang, Y.; Zhang, Z.; He, Q.; Lü, S.; Chen, J.; Saunders, S.; Yu, J. Design and characterization of a smog chamber for studying gas-phase chemical mechanisms and aerosol formation. *Atmos. Meas. Tech.* **2014**, *7* (1), 301−313.

(26) Liu, T.; Wang, X.; Hu, Q.; Deng, W.; Zhang, Y.; Ding, X.; Fu, X.; Bernard, F.; Zhang, Z.; Lü, S.; He, Q.; Bi, X.; Chen, J.; Sun, Y.; Yu, J.; Peng, P.; Sheng, G.; Fu, J. Formation of secondary aerosols from gasoline vehicle exhaust when mixing with SO2. *Atmos. Chem. Phys.* **2016**, *16* (2), 675−689.

(27) Deng, W.; Hu, Q.; Liu, T.; Wang, X.; Zhang, Y.; Song, W.; Sun, Y.; Bi, X.; Yu, J.; Yang, W.; Huang, X.; Zhang, Z.; Huang, Z.; He, Q.; Mellouki, A.; George, C. Primary particulate emissions and secondary organic aerosol (SOA) formation from idling diesel vehicle exhaust in China. *Sci. Total Environ.* **2017**, *593*−*594*, 462−469.

(28) World vegetable oils supply and distribution, 2012/13-2016/17. Technical Report; U.S. Department of Agriculture: Washington, DC, 2017.

(29) Zhang, X.; Cappa, C. D.; Jathar, S. H.; McVay, R. C.; Ensberg, J. J.; Kleeman, M. J.; Seinfeld, J. H. Influence of vapor wall loss in

DOI: 10.1021/acs.estlett.7b00530
Environ. Sci. Technol. Lett. 2018, 5, 32−37

laboratory chambers on yields of secondary organic aerosol. *Proc. Natl. Acad. Sci. U. S. A.* **2014**, *111* (16), 5802−5807.
(30) Benfenati, E.; Pierucci, P.; Niego, D. A case study of indoor pollution by Chinese cooking. *Toxicol. Environ. Chem.* **1998**, *65* (1−4), 217−224.
(31) He, L. Y.; Lin, Y.; Huang, X. F.; Guo, S.; Xue, L.; Su, Q.; Hu, M.; Luan, S. J.; Zhang, Y. H. Characterization of high-resolution aerosol mass spectra of primary organic aerosol emissions from Chinese cooking and biomass burning. *Atmos. Chem. Phys.* **2010**, *10* (23), 11535−11543.
(32) Liu, T.; Wang, X.; Deng, W.; Hu, Q.; Ding, X.; Zhang, Y.; He, Q.; Zhang, Z.; Lü, S.; Bi, X.; Chen, J.; Yu, J. Secondary organic aerosol formation from photochemical aging of light-duty gasoline vehicle exhausts in a smog chamber. *Atmos. Chem. Phys.* **2015**, *15* (15), 9049−9062.
(33) Ng, N. L.; Kroll, J. H.; Chan, A. W. H.; Chhabra, P. S.; Flagan, R. C.; Seinfeld, J. H. Secondary organic aerosol formation from m-xylene, toluene, and benzene. *Atmos. Chem. Phys.* **2007**, *7* (14), 3909−3922.
(34) Gordon, T. D.; Presto, A. A.; May, A. A.; Nguyen, N. T.; Lipsky, E. M.; Donahue, N. M.; Gutierrez, A.; Zhang, M.; Maddox, C.; Rieger, P.; Chattopadhyay, S.; Maldonado, H.; Maricq, M. M.; Robinson, A. L. Secondary organic aerosol formation exceeds primary particulate matter emissions for light-duty gasoline vehicles. *Atmos. Chem. Phys.* **2014**, *14* (9), 4661−4678.
(35) Lindinger, W.; Hansel, A.; Jordan, A. On-line monitoring of volatile organic compounds at pptv levels by means of proton-transfer-reaction mass spectrometry (PTR-MS) medical applications, food control and environmental research. *Int. J. Mass Spectrom. Ion Processes* **1998**, *173* (3), 191−241.
(36) Jordan, A.; Haidacher, S.; Hanel, G.; Hartungen, E.; Mark, L.; Seehauser, H.; Schottkowsky, R.; Sulzer, P.; Mark, T. D. A high resolution and high sensitivity proton-transfer-reaction time-of-flight mass spectrometer (PTR-TOF-MS). *Int. J. Mass Spectrom.* **2009**, *286* (2−3), 122−128.
(37) Hu, W.; Zhang, L.; Li, P.; Wang, X.; Zhang, Q.; Xu, B.; Sun, X.; Ma, F.; Ding, X. Characterization of volatile components in four vegetable oils by headspace two-dimensional comprehensive chromatography time-of-flight mass spectrometry. *Talanta* **2014**, *129*, 629−635.
(38) Buhr, K.; van Ruth, S.; Delahunty, C. Analysis of volatile flavour compounds by Proton Transfer Reaction-Mass Spectrometry: fragmentation patterns and discrimination between isobaric and isomeric compounds. *Int. J. Mass Spectrom.* **2002**, *221* (1), 1−7.
(39) DeCarlo, P. F.; Kimmel, J. R.; Trimborn, A.; Northway, M. J.; Jayne, J. T.; Aiken, A. C.; Gonin, M.; Fuhrer, K.; Horvath, T.; Docherty, K. S.; Worsnop, D. R.; Jimenez, J. L. Field-Deployable, High-Resolution, Time-of-Flight Aerosol Mass Spectrometer. *Anal. Chem.* **2006**, *78* (24), 8281−8289.
(40) Farmer, D. K.; Matsunaga, A.; Docherty, K. S.; Surratt, J. D.; Seinfeld, J. H.; Ziemann, P. J.; Jimenez, J. L. Response of an aerosol mass spectrometer to organonitrates and organosulfates and implications for atmospheric chemistry. *Proc. Natl. Acad. Sci. U. S. A.* **2010**, *107* (15), 6670−6675.
(41) Weitkamp, E. A.; Sage, A. M.; Pierce, J. R.; Donahue, N. M.; Robinson, A. L. Organic Aerosol Formation from Photochemical Oxidation of Diesel Exhaust in a Smog Chamber. *Environ. Sci. Technol.* **2007**, *41* (20), 6969−6975.
(42) Hildebrandt, L.; Donahue, N. M.; Pandis, S. N. High formation of secondary organic aerosol from the photo-oxidation of toluene. *Atmos. Chem. Phys.* **2009**, *9* (9), 2973−2986.
(43) Zhao, Y.; Saleh, R.; Saliba, G.; Presto, A. A.; Gordon, T. D.; Drozd, G. T.; Goldstein, A. H.; Donahue, N. M.; Robinson, A. L. Reducing secondary organic aerosol formation from gasoline vehicle exhaust. *Proc. Natl. Acad. Sci. U. S. A.* **2017**, *114* (27), 6984−6989.
(44) Chacon-Madrid, H. J.; Donahue, N. M. Fragmentation vs. functionalization: chemical aging and organic aerosol formation. *Atmos. Chem. Phys.* **2011**, *11* (20), 10553−10563.
(45) Trump, E. R.; Epstein, S. A.; Riipinen, I.; Donahue, N. M. Wall effects in smog chamber experiments: A model study. *Aerosol Sci. Technol.* **2016**, *50* (11), 1180−1200.
(46) Liu, T.; Liu, Q.; Li, Z.; Huo, L.; Chan, M.; Li, X.; Zhou, Z.; Chan, C. K. Emission of volatile organic compounds and production of secondary organic aerosol from stir-frying spices. *Sci. Total Environ.* **2017**, *599−600*, 1614−1621.
(47) Choe, E.; Min, D. B. Mechanisms and Factors for Edible Oil Oxidation. *Compr. Rev. Food Sci. Food Saf.* **2006**, *5* (4), 169−186.
(48) Mao, J.; Ren, X.; Brune, W. H.; Olson, J. R.; Crawford, J. H.; Fried, A.; Huey, L. G.; Cohen, R. C.; Heikes, B.; Singh, H. B.; Blake, D. R.; Sachse, G. W.; Diskin, G. S.; Hall, S. R.; Shetter, R. E. Airborne measurement of OH reactivity during INTEX-B. *Atmos. Chem. Phys.* **2009**, *9* (1), 163−173.
(49) Chan, A. W. H.; Chan, M. N.; Surratt, J. D.; Chhabra, P. S.; Loza, C. L.; Crounse, J. D.; Yee, L. D.; Flagan, R. C.; Wennberg, P. O.; Seinfeld, J. H. Role of aldehyde chemistry and NOx concentrations in secondary organic aerosol formation. *Atmos. Chem. Phys.* **2010**, *10* (15), 7169−7188.
(50) Chhabra, P. S.; Ng, N. L.; Canagaratna, M. R.; Corrigan, A. L.; Russell, L. M.; Worsnop, D. R.; Flagan, R. C.; Seinfeld, J. H. Elemental composition and oxidation of chamber organic aerosol. *Atmos. Chem. Phys.* **2011**, *11* (17), 8827−8845.
(51) Chacon-Madrid, H. J.; Presto, A. A.; Donahue, N. M. Functionalization vs. fragmentation: n-aldehyde oxidation mechanisms and secondary organic aerosol formation. *Phys. Chem. Chem. Phys.* **2010**, *12* (42), 13975−13982.
(52) Grieshop, A. P.; Logue, J. M.; Donahue, N. M.; Robinson, A. L. Laboratory investigation of photochemical oxidation of organic aerosol from wood fires 1: measurement and simulation of organic aerosol evolution. *Atmos. Chem. Phys.* **2009**, *9* (4), 1263−1277.
(53) Jathar, S. H.; Gordon, T. D.; Hennigan, C. J.; Pye, H. O. T.; Pouliot, G.; Adams, P. J.; Donahue, N. M.; Robinson, A. L. Unspeciated organic emissions from combustion sources and their influence on the secondary organic aerosol budget in the United States. *Proc. Natl. Acad. Sci. U. S. A.* **2014**, *111* (29), 10473−10478.
(54) Robinson, A. L.; Donahue, N. M.; Shrivastava, M. K.; Weitkamp, E. A.; Sage, A. M.; Grieshop, A. P.; Lane, T. E.; Pierce, J. R.; Pandis, S. N. Rethinking Organic Aerosols: Semivolatile Emissions and Photochemical Aging. *Science* **2007**, *315* (5816), 1259−1262.
(55) Zhao, Y.; Nguyen, N. T.; Presto, A. A.; Hennigan, C. J.; May, A. A.; Robinson, A. L. Intermediate Volatility Organic Compound Emissions from On-Road Diesel Vehicles: Chemical Composition, Emission Factors, and Estimated Secondary Organic Aerosol Production. *Environ. Sci. Technol.* **2015**, *49* (19), 11516−11526.

DOI: 10.1021/acs.estlett.7b00530
Environ. Sci. Technol. Lett. 2018, 5, 32−37